ROS

RESEARCH ARTICLES

Chronic Intermittent Hypoxia Causes Lipid Peroxidation and Altered Phase 1 Drug Metabolizing Enzymes in the Neonatal Rat Liver

Charles Cai[1], Jacob V. Aranda[1–3], Gloria B. Valencia[1], Jiliu Xu[4], and Kay D. Beharry[1–3].

[1]Department of Pediatrics, Division of Neonatal-Perinatal Medicine, State University of New York, Downstate Medical Center, Brooklyn, NY 11203, USA; [2]Department of Ophthalmology, State University of New York, Downstate Medical Center, Brooklyn, NY 11203, USA; [3]SUNY Eye Institute, New York, NY 13202, USA; [4]Department of Pediatrics, Division of Gastroenterology, State University of New York, Downstate Medical Center, Brooklyn, NY 11203, USA

Correspondence: kbeharry@downstate.edu (K.D.B.)

Cai C et al. Reactive Oxygen Species 3(9):218–236, 2017; ©2017 Cell Med Press
http://dx.doi.org/10.20455/ros.2017.835
(Received: March 30, 2017; Revised: April 11, 2017; Accepted: April 12, 2017)

ABSTRACT | Critically ill preterm neonates requiring oxygen therapy often experience frequent apneas with intermittent hypoxia (IH). IH-induced oxidative stress causes lipid peroxidation, which targets the liver and contributes to toxic drug reactions. We tested the hypothesis that incremental IH episodes induce oxidative damage in the neonatal liver and alter the expression of genes that regulate drug metabolism. Newborn rats were exposed to increasing IH episodes (12% O_2) during hyperoxia (50% O_2), or placed in room air (RA) until postnatal day 21 (P21) for recovery from IH (IHR). RA littermates served as controls, and pups exposed to 50% O_2 served as hyperoxia controls. Hepatic histopathology, biomarkers of oxidative stress and oxidative DNA damage, antioxidants, and expression of genes that regulate drug metabolism were assessed. Oxidative stress and DNA damage, evidenced by 8-isoprostaglandin $F_{2\alpha}$ (8-isoPGF$_{2\alpha}$) and 8-hydroxy-2′-deoxyguanosine (8-OH-dG), respectively, increased as a function of IH episodes, and was associated with decreased superoxide dismutase (SOD) and increased catalase activities. Pathological changes including cellular swelling, steatosis, necrosis, and focal sinusoid congestion were seen in IH, but not in IHR. Similarly, IH was associated with upregulation of several genes involved in DNA repair, which were downregulated during IHR. Of the genes involved in drug metabolism, aldehyde dehydrogenases (involved in lipid peroxidation) and cytochrome P450 (CYP) genes of the 2C family (involved in oxidative stress) were robustly upregulated both in IH and in IHR. Hepatic oxidative stress and lipid peroxidation occurring in response to chronic IH have implications for preterm infants, and may explain, in part, the pharmacokinetic variations and drug toxicities in this vulnerable population.

KEYWORDS | DNA damage; Hyperoxia; Intermittent hypoxia; Lipid peroxidation; Liver; Oxidative stress; Neonatal rat

ABBREVIATIONS | AOP, apnea of prematurity; CYP, cytochrome P450; ELBW, extremely low birth weight; ELGAN, extremely low gestational age neonate; GPx, glutathione peroxidase; IF,

immunofluorescence; IH, intermittent hypoxia; IHR, recovery from IH; 8-isoPGF$_{2\alpha}$, 8-isoprostaglandin F$_{2\alpha}$; NSAID, non-steroidal anti-inflammatory drug; 8-OH-dG, 8-hydroxy-2′-deoxyguanosine; RA, room air; ROS, reactive oxygen species; SOD, superoxide dismutase

CONTENTS

1. Introduction
2. Material and Methods
   2.1. Experimental Design
   2.2. IH Cycling
   2.3. Oxidative Stress and DNA Damage
   2.4. Antioxidant Activities
   2.5. Total Cellular Protein Assay
   2.6. Hematoxylin and Eosin (H&E) Staining
   2.7. Immunofluorescence Staining
   2.8. Oxidative Stress and Phase 1 Metabolizing Genes
   2.9. Statistical Analyses
3. Results
   3.1. Liver 8-isoPGF2α and 8-OH-dG
   3.2. Liver Antioxidant Activities
   3.3. Liver Histopathology
   3.4. Liver Immunofluorescence of CYP Isozymes
   3.5. Genes Regulating DNA Damage and Repair
   3.6. Phase 1 Metabolizing Genes
4. Discussion

1. INTRODUCTION

Liver dysfunction, clinically manifested by hyperbilirubinemia, affects as many as 50% of extremely low gestational age neonates (ELGANs) and extremely low birthweight (ELBW) infants [1]. Despite multifactorial in etiology, hypoxia/ischemia has been considered one of the major risk factors contributing to hepatic dysfunction in these infants [2]. One of the serious long-term adverse effects associated with early onset liver diseases in ELGANS is an intellectual impairment [3], thus highlighting the need for further mechanistic studies of hypoxia-induced liver injury in neonates. Apnea of prematurity (AOP) with intermittent hypoxia (IH), is a major problem in ELGANS and ELBW infants. The incidence of AOP varies with the degree of prematurity, from 7% at 34–35 weeks of gestational age to 15% at 32–33 weeks, 54% at 30–31 weeks, and nearly 100% at < 28 weeks [4]. Apneas of less than 10 seconds duration can result in a reduction in oxygen saturation of 40% [4]. Studies have shown that ELGANs experience as many as 600 IH episodes per week during the first few weeks of life [5–8]. These IH events can lead to oxidative stress, which may underpin many of the diseases of the preterm neonate.

Compared to older children and adults, ELGANs are more susceptible to oxidative injury mediated by accumulation of reactive oxygen species (ROS). This is largely due to reduced antioxidant defenses [9–11]. ELGANs often receive iron supplementation for iron deficiency [12–15]. Excessive free iron reacts with hydrogen peroxide (H_2O_2), one of the most abundant ROS, by the Fenton and Haber–Weis reactions to form the highly toxic hydroxyl radical [16, 17]. The main ROS produced is superoxide anion which is short-lived as it is rapidly degraded to H_2O_2 and O_2 by superoxide dismutase (SOD), the first line of defense [18, 19]. Induction of other antioxidants such as mitochondrial glutathione peroxidase (GPx) and catalase follows to scavenge and detoxify H_2O_2 in the mitochondria and cytosol. In ELGANS, however, these antioxidant responses are compromised. The H_2O_2, accumulated from excessive formation

and limited clearance, reacts with free iron to form the more reactive from of ROS, hydroxyl radical, which further targets lipids and DNA for oxidative damage [20–23]. The imbalance between ROS overproduction and antioxidant defenses is of particular significance in the liver due to its high susceptibility to lipid peroxidation [20–23].

The liver is a prominent organ in neonates. It constitutes approximately 5% of the body weight at birth (compared to 2% in adults) with a large volume (per unit of body weight) of 48 ml/kg [24]. Exposure of the preterm liver to chronic IH can also impair metabolism of many drugs that ELGANs are exposed to including caffeine for AOP, non-steroidal anti-inflammatory drugs (NSAIDs) for closure of a symptomatic patent ductus arteriosus, and antibiotics, among others [23, 25–27]. ELGANs have shown variable pharmacokinetic profiles of many drugs likely due to immature cytochrome P450 (CYP) system [28–30]. The combined effects of IH, ROS, and immature drug metabolizing enzymes can contribute to severe hepatotoxicity. Studies show that H_2O_2 and other ROS diminish hepatic expression and activity of CYP enzymes [31–36].

Based upon these reports, we tested the hypothesis that increasing episodes of IH followed by IHR cause substantial ROS damage to the liver and alter the expression of phase 1 drug metabolizing enzymes. To prove this hypothesis, we exposed neonatal rats to increasing episodes of neonatal IH and examined the responses of hepatic biomarkers of oxidative stress, oxidative DNA damage, antioxidants, and CYP gene expression.

2. MATERIAL AND METHODS

All experiments were approved by the State University of New York, Downstate Medical Center Institutional Animal Care and Use Committee, Brooklyn, NY, USA. Animals were treated humanely, according to the guidelines outlined by the United States Department of Agriculture and the Guide for the Care and Use of Laboratory Animals.

2.1. Experimental Design

Certified infection-free, timed-pregnant Sprague Dawley rats were purchased from Charles River Laboratories (Wilmington, MA, USA) at 17 days of gestation. The animals were housed in an animal facility with a 12-hour-day/12-hour-night cycle and provided standard laboratory diet and water ad libitum until delivery. Within 2–3 hours of birth, newborn pups delivered on the same day were pooled and randomly assigned to expanded litters of 18 pups/litter (9 males and 9 females). Gender was determined by the anogenital distance. The expanded litter size was used to simulate relative postnatal malnutrition of critically ill ELGANs. Each pup was weighed and measured for linear growth (crown to rump length in centimeters). A total of 31 groups of 18 rat pups (9 males and 9 females) were studied according to the experimental design previously published [34].

The groups are described as follows: (1) groups 1 to 6 were exposed to 2, 4, 6, 8, 10, or 12 IH cycling episodes from P0 to P7; (2) groups 7 to 12 were exposed to 2, 4, 6, 8, 10, or 12 IH cycling episodes from P0 to P14; (3) groups 13 to 18 were exposed to 2, 4, 6, 8, 10, or 12 IH cycling episodes from P0 to P7, followed by re-oxygenation in room air (RA) for 14 days from P7 to P21; (4) groups 18 to 24 were exposed to 2, 4, 6, 8, 10, or 12 IH cycling episodes from P0 to P14, followed by re-oxygenation in RA for 7 days from P14 to P21; (5) groups 25 to 28 were exposed to 50% O_2 only for 7 days, 14 days, 7 days with 14 days of re-oxygenation in RA, or 14 days with 7 days of re-oxygenation in RA. These served as O_2 controls, or zero IH; and (6) groups 29–31 were littermates raised in RA from birth to P7, P14, or P21 with all conditions identical except for atmospheric oxygen and served as RA controls.

2.2. IH Cycling

The IH cycles consisted of hyperoxia (50% O_2)/hypoxia (12% O_2) in stepwise increments of brief (1 min), hypoxia (12%) clusters (3 clusters) during 50% O_2 for a total of 2, 4, 6, 8, 10, or 12 episodes/day. This clustering design has been shown to produce severe oxidative stress in neonatal rats [35–40]. There were two IH groups corresponding to 7-day (P0–P7), and 14-day (P0–P14). To determine the immediate effects, animals were euthanized on P7 or P14. To determine the effects of IHR, all animals were euthanized on P21 after either 14 days of recovery in RA following 7-day IH (P7–P21), or 7 days of recovery in RA following 14-day IH (P14–P21).

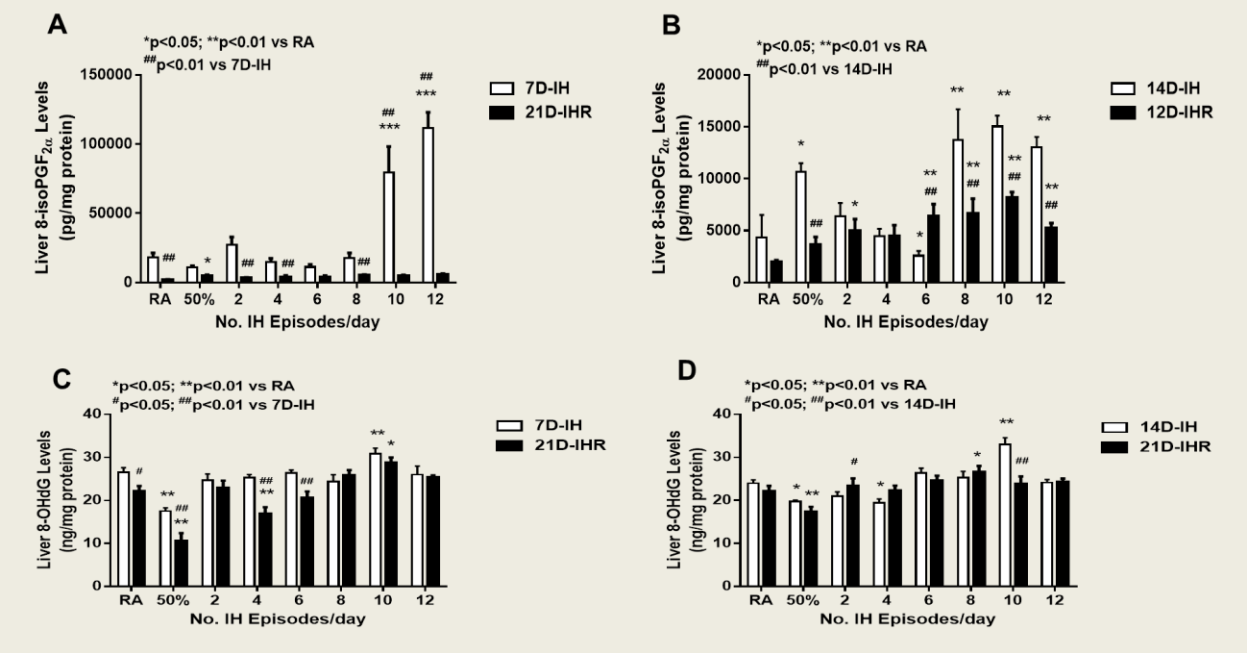

FIGURE 1. Effects of incremental IH episodes on 8-isoPGF$_{2\alpha}$ (A, B) and 8-OH-dG (C, D) in the liver of neonatal rats at P7 (7D-IH), P14 (14D-IH), or P21-IHR. Animals recovering from 7D-IH were placed in RA from P7–P21 and animals recovering from 14D-IH were placed in RA from P14–P21. Animals randomized to IH were exposed to brief clustered IH episodes during 50% O_2. Animals randomized to hyperoxia were exposed to 50% O_2 only. RA controls remained in atmospheric O_2. Data are presented as mean ± SEM (n=8 samples/group).

2.3. Oxidative Stress and DNA Damage

8-Isoprostane (8-isoPGF$_{2\alpha}$) is commonly studied and abundantly generated in vivo during oxidative stress and lipid peroxidation. To establish ocular oxidative stress and DNA damage, levels of 8-isoPGF$_{2\alpha}$ and 8-hydroxy-2′-deoxyguanosine (8-OH-dG), respectively, were determined in the liver homogenates using commercially-available enzyme immunoassay kits (Assay Designs, Ann Arbor, MI, USA), according to the manufacturer's protocol. Levels in the homogenates were standardized using total cellular protein levels according to the Bradford method (Bio-Rad, Hercules, CA, USA).

2.4. Antioxidant Activities

Superoxide dismutase (SOD), catalase activities were determined in the homogenates using commercially-available assay kits (Cayman Chemicals, Ann Arbor, MI, USA) according to the manufacturer's protocol. The SOD and catalase activities were determined spectrophotometrically at 450 nm and 540 nm, respectively. Levels were standardized using total cellular protein levels.

2.5. Total Cellular Protein Assay

On the day of the assay, liver homogenates were assayed for total protein levels using the dye-binding Bio-Rad protein assay kit (Bio-Rad, Hercules, CA, USA) with bovine serum albumin as a standard.

2.6. Haemotoxylin and Eosin (H & E) Staining

Liver biopsies were fixed in 10% neutral buffered formalin (NBF) and sent to Histowiz (Brooklyn, NY, USA) for processing, sectioning, and H&E staining. Images were captured at 40× magnification using an Olympus BX53 microscope, DP72 digital camera, and

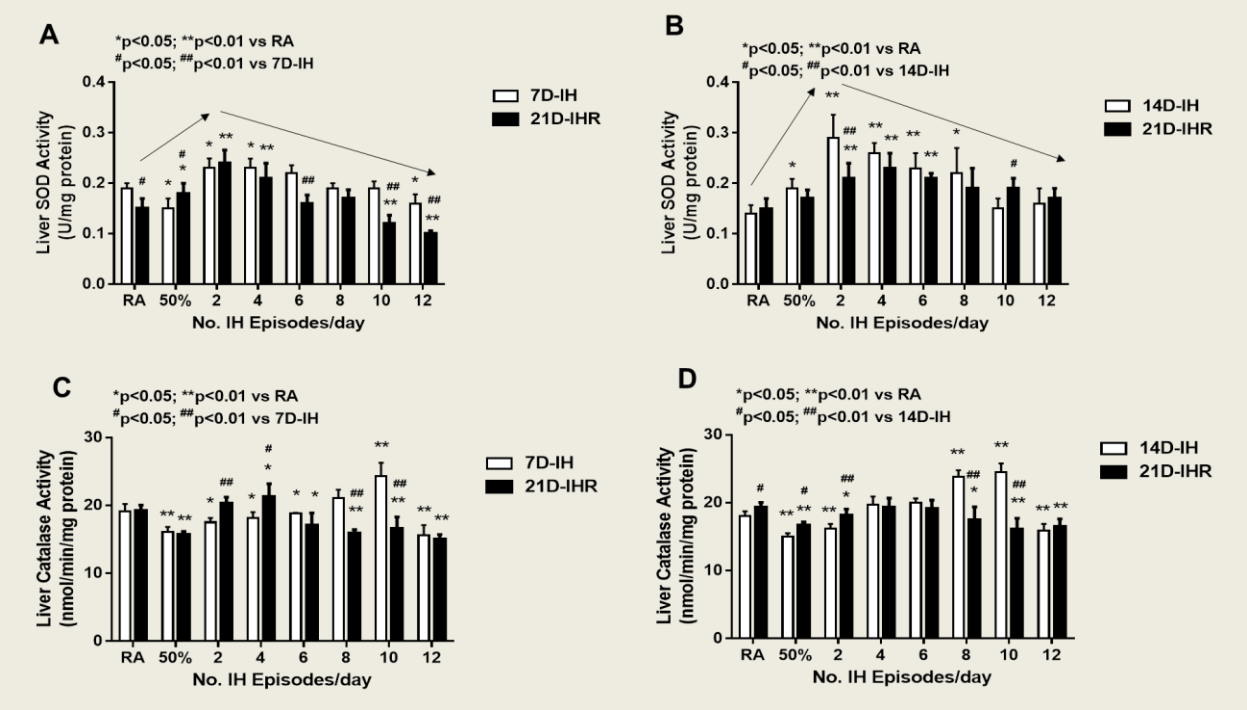

FIGURE 2. Effects of incremental IH episodes on SOD (A, B) and catalase (C, D) activities in the liver of neonatal rats at P7 (7D-IH), P14 (14D-IH), or P21-IHR. Animals recovering from 7D-IH were placed in RA from P7–P21 and animals recovering from 14D-IH were placed in RA from P14–P21. Animals randomized to IH were exposed to brief clustered IH episodes during 50% O_2. Animals randomized to hyperoxia were exposed to 50% O_2 only. RA controls remained in atmospheric O_2. Data are presented as mean ± SEM (n=8 samples/group).

CellSens imaging software (Olympus, Center Valley, PA, USA), attached to a Dell Precision T3500 computer (Dell, Round Rock, TX, USA). Unstained sections were used for immunofluorescence staining of CYP1A2 and CYP2D6.

2.7. Immunofluorescence Staining

Unstained sections were de-paraffinized and treated with xylenes and ethanol. The slides were placed in 10 mM sodium citrate buffer, pH 6.0 and heated at 95–100°C for 20 minutes to unmask the antigens. Following several washes, Immunofluorescence staining **(**IF) staining was conducted using primary antibodies (Santa Cruz Biotechnology, Dallas, TX, USA) and Alexa Fluor fluorescent secondary antibodies (Life Technologies, Grand Island, NY, USA). All IF protocols were conducted according to the manufacturer's recommendations. IF sections were imaged at 40× magnification using an Olympus BX53 microscope, DP72 digital camera, and CellSens imaging software (Olympus, Center Valley, PA, USA), attached to a Dell Precision T3500 computer (Dell, Round Rock, TX, USA).

2.8. Oxidative Stress and Phase 1 Metabolizing Genes

Total RNA was extracted as previously described [39–41]. Real-time polymerase chain reaction (PCR) arrays were carried out in duplicate using the rat oxidative stress and phase 1 metabolizing gene arrays (Qiagen, Germantown, MD, USA) with a Bio-Rad IQ5 real-time instrument (Bio-Rad, Hercules, CA, USA) according to the manufacturers' protocols.

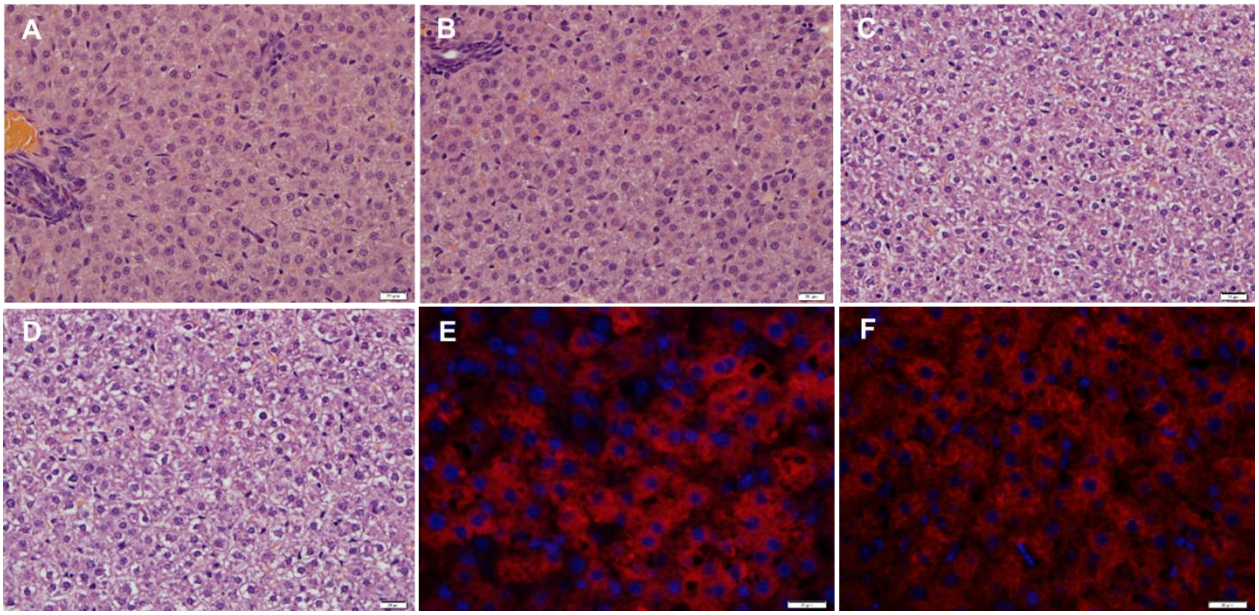

FIGURE 3. Representative H & E stain of liver sections from RA controls at P7 (A), P14 (B) and P21 (C and D), and representative immunofluorescence stain of CYP1A2 (E) and CYP2D6 (F) from RA controls at P21. Control liver sections show normal architecture and robust immunostaining in the hepatocytes. Images are 40× magnification. Scare bar represents 20 μm.

2.9. Statistical Analyses

Data were analyzed in two ways: (1) comparison of 50% O_2 and IH groups to RA; and (2) comparison IH to IHR. A test for normality was conducted using the Bartlett's test, prior to all statistical analyses. Normally distributed data was analyzed using two-way analysis of variance with Bonferroni post-hoc tests. Non-normally distributed data was analyzed using Kruskall Wallis test with Dunn's multiple comparison test. Data are presented as mean ± SEM (n = 8) and a p value of < 0.05 was considered as statistically significant, using SPSS version 16.0 (SPSS, Chicago, IL, USA) and graphs were prepared using GraphPad Prizm (GraphPad, San Diego, CA, USA).

3. RESULTS

3.1. Liver 8-isoPGF$_{2\alpha}$ and 8-OH-dG

Figure 1 represents the effects of increasing IH episodes (white bar) and subsequent IHR (black bar) on 8-isoPGF$_{2\alpha}$ and 8-OH-dG in neonatal rat liver homogenates. In the 7-day IH groups, the levels of 8-isoPGF$_{2\alpha}$ were substantially higher compared to the IHR groups. Exposure to 10 and 12 IH episodes per day evoked a profound increase in liver 8-isoPGF$_{2\alpha}$ levels. IHR for 14 days resulted in consistently lower 8-isoPGF$_{2\alpha}$ levels with a moderate increase in the hyperoxia group compared to RA (**Figure 1A**). Exposure to 14-day IH resulted in higher 8-isoPGF$_{2\alpha}$ with 8–12 IH episodes, as did exposure to hyperoxia alone. While IHR for 7 days following either hyperoxia or IH decreased 8-isoPGF$_{2\alpha}$ levels, IHR following 6 IH episodes caused an increase (**Figure 1B**). In the 7-day IH groups, liver 8-OH-dG levels decreased with hyperoxia only and progressively increased with the number of IH episodes to peak with 10 IH episodes. In the 14-day IHR groups the levels declined in the hyperoxia groups and groups exposed to 4, 6, and 10 IH groups (**Figure 1C**). In the 14-day IH groups, the effects on 8-OH-dG appeared to be also lower with hyperoxia, but to a lesser degree, and peaked with 10 IH episodes. IHR was lower in the 10 IH group only, compared to IH (**Figure 1D**).

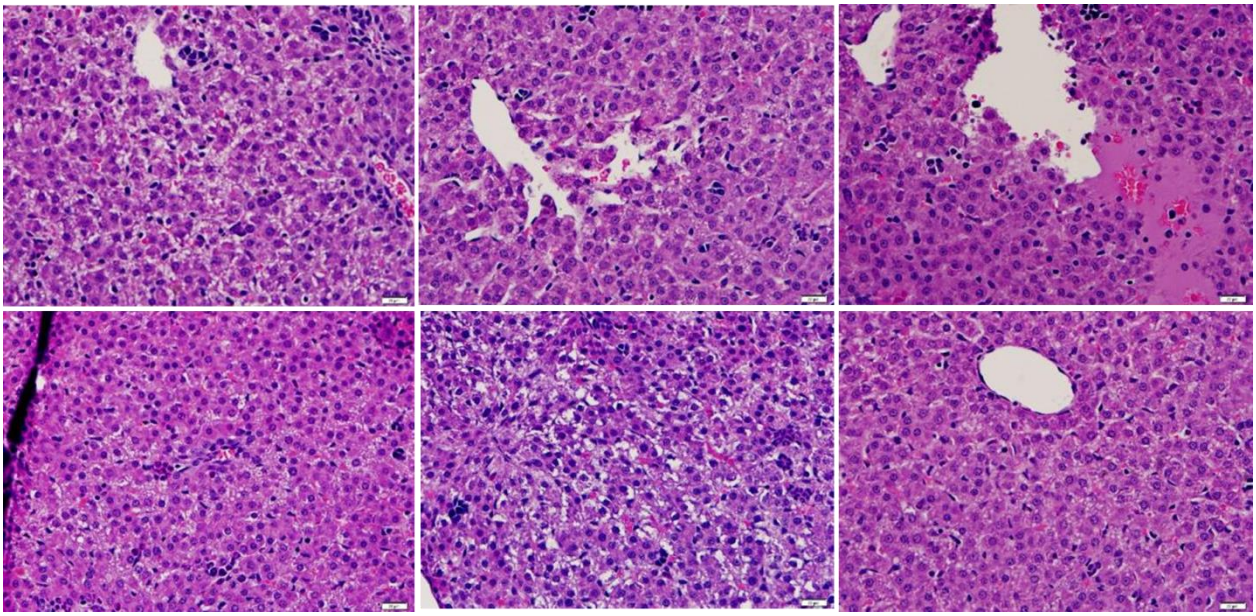

FIGURE 4. Representative H & E stain of liver sections from 7D-IH groups exposed to 2 (A), 4 (B), 6 (C), 8 (D), 10 (E), and 12 (F) IH episodes per day. Increasing episodes of IH caused cellular swelling, steatosis, necrosis and focal sinusoid congestion starting as early as 2 IH episodes per day (arrows). More severe apoptosis occurred with 6 IH episodes per day. No major damage was seen with 8 and 12 IH episodes. Images are 40× magnification. Scare bar represents 20 µm.

3.2. Liver Antioxidant Activities

Figure 2 represents the effects of increasing IH episodes (white bar) and subsequent IHR (black bar) on SOD (A and B) and catalase (C and D) activities in the liver homogenates. In the 7-day IH group, liver SOD activities were highest with 2 IH episodes per day and progressively declined with 4–12 IH episodes per day. IHR following 7-day IH exposure followed a similar pattern and were lower than IH levels with 8, 10, and 12 IH episodes (**Figure 2A**). Exposure to chronic IH (14-day) episodes displayed a similar pattern to 7-day IH exposure, but with a higher peak production with 2 IH episodes, although lower levels were found with recovery compared to IH (**Figure 2B**). In the 7-day IH group, liver catalase levels declined with hyperoxia and with 2–6, and 12 IH episodes. Exposure to 10 IH episodes increased catalase levels. During IHR, the levels were higher with 2 and 4 IH episodes, and lower with 6–12 IH episodes. Catalase levels did not change during recovery from hyperoxia (**Figure 2C**). Exposure to long-term IH caused significant increases in catalase with 8 and 10 episodes. Both hyperoxia and 12 IH episodes caused lower catalase levels. During IHR, catalase levels remained consistently lower in the hyperoxia group and in the 8–10 IH groups (**Figure 2D**).

3.3. Liver Histopathology

Figure 3 shows normal histology of liver tissue from RA animals at P7 (A), P14 (B), and P21 (C and D). **Figure 4** shows liver sections from animals exposed to 7 days of 2 (A), 4 (B), 6 (C), 8 (D), 10 (E), and 12 (F) IH episodes per day. Increasing episodes of IH caused cellular swelling, steatosis, necrosis and focal sinusoid congestion starting as early as 2 IH episodes per day. More severe apoptosis occurred with 6 IH episodes per day. No major damage was seen with 8 and 12 IH episodes. **Figure 5** shows liver sections from animals exposed to 14 days of 2 (A), 4 (B), 6 (C), 8 (D), 10 (E), and 12 (F) IH episodes per day. While the damage was less severe than that seen af-

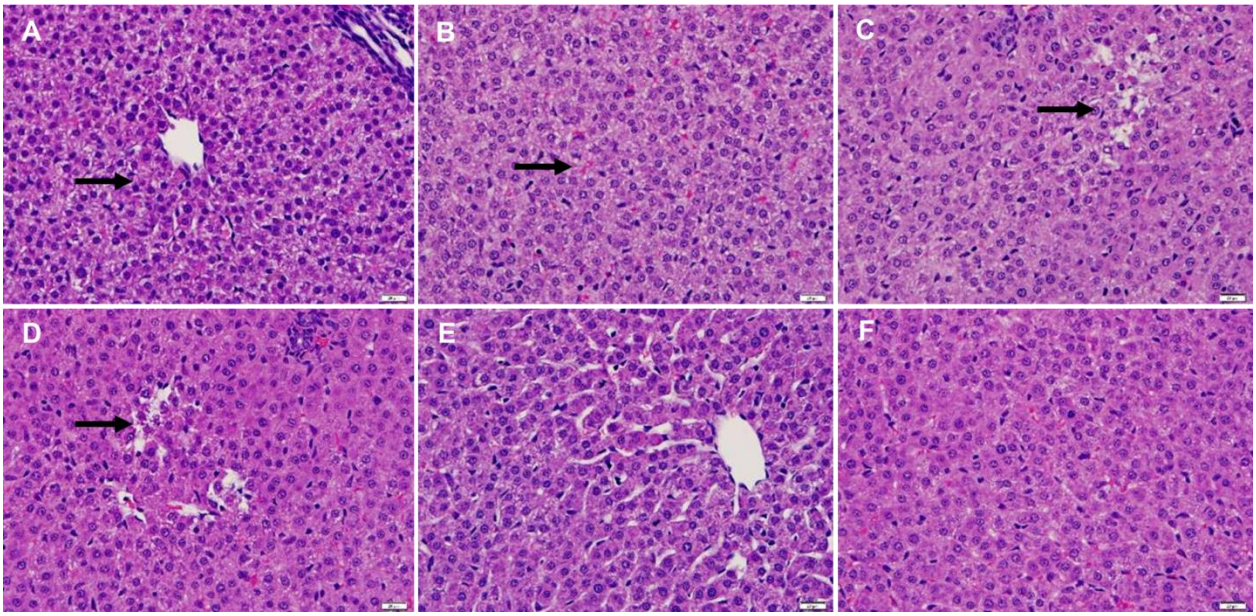

FIGURE 5. Representative H & E stain of liver sections from 14D-IH groups exposed to 2 (A), 4 (B), 6 (C), 8 (D), 10 (E), and 12 (F) IH episodes per day. Images show evidence of necrosis and steatosis in the groups exposed to 6-10 IH episodes (arrows). Exposure to 12 IH episodes showed evidence of blood sinusoid dilation and hemorrhage (arrows). Images are 40× magnification. Scare bar represents 20 μm.

ter 7 days of IH exposure, there was evidence of necrosis and steatosis in the groups exposed to 6–10 IH episodes. Exposure to 12 IH episodes showed evidence of blood sinusoid dilation and hemorrhage. **Figure 6** shows liver sections from animals exposed to 7 days of 2 (A), 4 (B), 6 (C), 8 (D), 10 (E), and 12 (F) IH episodes per day with 14 days of IHR. IHR in all groups showed no major evidence of necrosis, but cytoplasmic vacuolization, pervasive steatosis, blood sinusoid dilation and hemorrhage occurred particularly in the 12 IH/IHR group. **Figure 7** shows liver sections from animals exposed to 14 days of 2 (A), 4 (B), 6 (C), 8 (D), 10 (E), and 12 (F) IH episodes per day with 7 days of IHR. IHR in all groups showed no major evidence of necrosis, but similar to the 14-day IHR groups, there was pervasive steatosis, blood sinusoid dilation, hemorrhage, and cytoplasmic vacuolization.

3.4. Liver Immunofluorescence of CYP Isozymes

Figure 3E and **3D** shows expression of CYP1A2 and CYP2D6, respectively in hepatocytes of livers from control rats at P21. **Figures 8** and **9** shows significantly reduced intensity in all groups exposed to 14 days of IH with 7 days of IHR, although CYP1A2 was moderately expressed in the group exposed to 2 IH episodes per day (**Figure 8A**).

3.5. Genes Regulating DNA Damage and Repair

Expression of genes regulating DNA damage and repair after 14 days of IH is presented in **Table 1**, and the expression of the same genes after 14 days of IH and 7 days IHR are presented in **Table 2**. Data are expressed as fold changes as compared to P14 or P21 RA controls. A total of 18 genes are selected from a panel of 84 genes involved in the regulation of DNA damage, DNA repair, apoptosis, and cell cycle. Samples from 4–10 IH episodes for 14 days and the corresponding IHR at 21 days are presented to correlate with data from **Figures 1** and **2**. Concurrent with the results shown in **Figures 1** and **2**, exposure to IH resulted in higher expression of genes compared to IHR. During IHR, most genes remained downregulated.

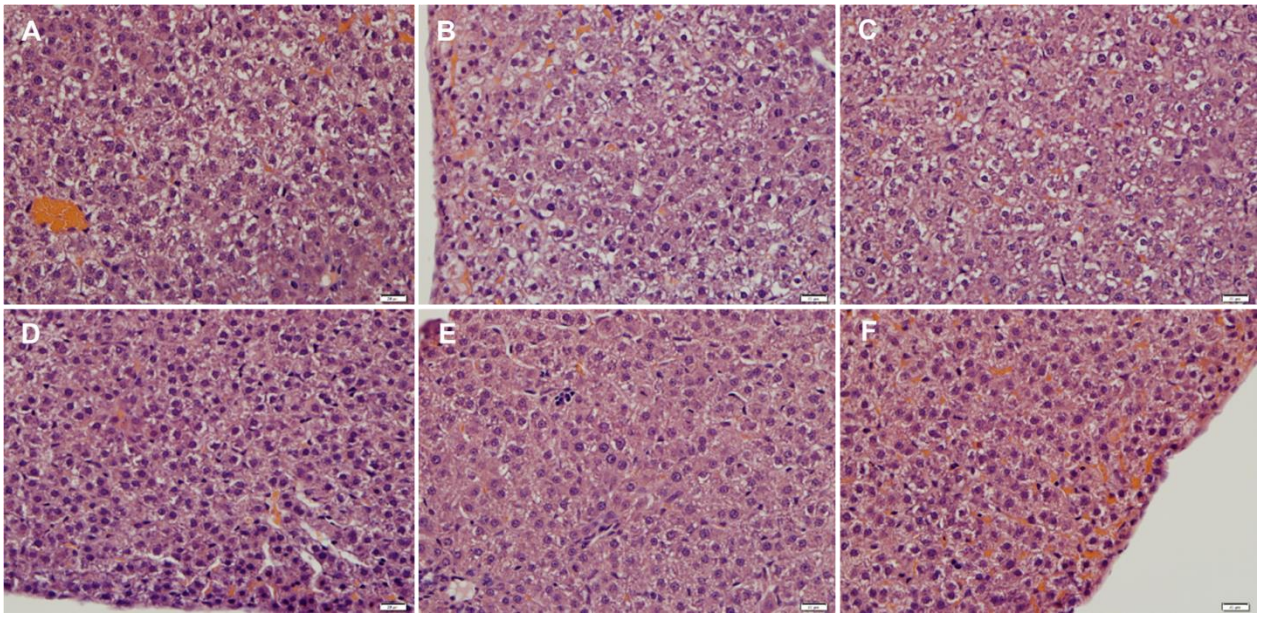

FIGURE 6. Representative H & E stain of liver sections from 21-day old rats exposed to 7 days of IH and 14 days of IHR, and exposed to 2 (A), 4 (B), 6 (C), 8 (D), 10 (E), and 12 (F) IH episodes per day. IHR in all groups showed no major evidence of necrosis, but there was and cytoplasmic vacuolization, pervasive steatosis, blood sinusoid dilation and hemorrhage, particularly in the 12 IH/IHR group (arrows). Images are 40× magnification. Scare bar represents 20 µm.

3.6. Phase 1 Metabolizing Genes

Expression of genes encoding proteins that are involved in phase 1 drug metabolism following 14 days of IH and 7 days of IHR are presented in **Tables 3** and **4**, respectively. A total of 22 genes are selected from a panel of 84 genes. Aldehyde dehydrogenase genes, most notably Aldh6 (139-fold upregulation), were several fold upregulated with 10 IH episodes after 14 days of exposure, as was cycloxygenase-2 (COX-2), the inducible form of COX associated with inflammation. In contrast, most CYP genes, whose encoded proteins are flavin-containing monooxygenases, responsible for catalyzing the oxidation of many drugs, were downregulated with increasing IH episodes (**Table 3**). Compared to P14, expression of genes involved in phase 1 drug metabolism was substantially lower during IHR, except for Aldh2 (59-fold), Aldh6 (> 230-fold), inducible COX-2 (24-fold), the retinoid inducible Cyp2c22 (> 86-fold), Cyp2e1 (> 60-fold), and Fm05 (35-fold) which were robustly upregulated (**Table 4**).

4. DISCUSSION

The results of this study show that IH and subsequent IHR, inflict detrimental effects to the neonatal liver via oxidative stress and DNA damage. The importance of these findings relates specifically to the significant pharmacologic variations that exist among preterm neonates, as well as the substantial variation in pharmacokinetic profiles of drugs which is most likely due to immature drug metabolizing enzymes [28–30]. Since drug therapies in ELGANs are largely based on data from older children and adults, one important factor that has not been considered but may contribute to toxicokinetics and toxicodynamics in this vulnerable population, is the effect of IH on drug metabolizing enzymes.

Critically ill preterm neonates are exposed to a multitude of off-label drugs including methylxanthines, NSAIDs, antibiotics, narcotics, etc. for various morbidities. The combination of polypharmacy, recurring IH/IHR episodes, and immature and/or deficient drug metabolizing systems contribute to toxic

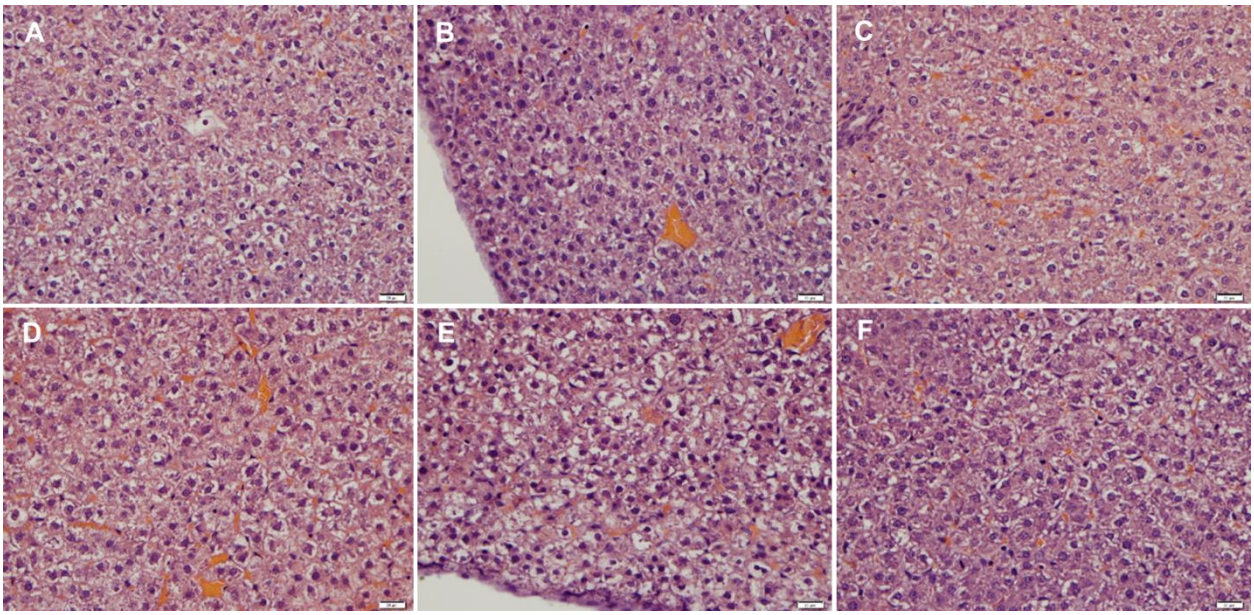

FIGURE 7. Representative H & E stain of liver sections from 21-day old rats exposed to 14 days of IH and 7 days of IHR, and exposed to 2 (A), 4 (B), 6 (C), 8 (D), 10 (E), and 12 (F) IH episodes per day. IHR in all groups showed no major evidence of necrosis, but similar to the 14-day IHR groups, there was pervasive steatosis, blood sinusoid dilation, hemorrhage, and cytoplasmic vacuolization (arrows). Images are 40× magnification. Scare bar represents 20 μm.

drug reaction. Drug metabolizing enzymes are divided into phase 1 and phase 2 enzymes. Phase 1 enzymes are involved primarily with oxidation, reduction and hydrolysis processes, while phase 2 enzymes conjugate drug molecules to allow excretion [41]. The most important group of enzymes involved in phase 1 metabolism are CYP enzymes. Deficient or immature activity of CYP enzymes can be responsible for the extreme toxicity seen in preterm neonates [42–44]. At birth, total neonatal hepatic CYP content is approximately 30% of adult levels [45], and increases at variable rates during the perinatal period [44–47]. CYP3A4 is responsible for the metabolism of a vast majority of currently marketed drugs. It is the most abundantly expressed CYP enzyme in the liver, accounting for 30–40% of total CYP enzyme content in the organ, and is functionally immature at birth reaching 50% of adult levels by 6–12 months of age [48]. In this study, we found no significant effects of IH on CYP3A4. This is likely due to the immature function of this CYP isozyme. Other metabolic deficiencies include decreased hydroxylating and esterase activities [49] and glucuronidation mechanisms [50].

The hepatic glucuronyltransferase system in the neonatal rat at birth is not fully developed. At day 14, it is functional at or close to maximal efficiency, and at 21 days postnatal age is functional at or close to adult capacity [51]. Using validated biomarkers for oxidative stress and DNA damage, 8-isoPGF$_{2\alpha}$ and 8-OH-dG, respectively [52, 53], we showed that IH causes oxidative stress and DNA damage to the liver. Oxidative stress was significantly more severe in the groups experiencing10 and 12 IH episodes per day despite the shorter hyperoxic events between IH episodes compared to the other groups. This clearly demonstrates that hypoxia can exert more oxidative damaging effects on the liver than hyperoxia. RA recovery is unable to appreciably mitigate the effects. Oxidative stress and propagation of ROS target the liver due to its high lipid content, resulting in lipid peroxidation [20–23]. Studies show that H_2O_2, as well as other ROS diminishes the expression, content, and activity of CYP isozymes [31]. In addition,

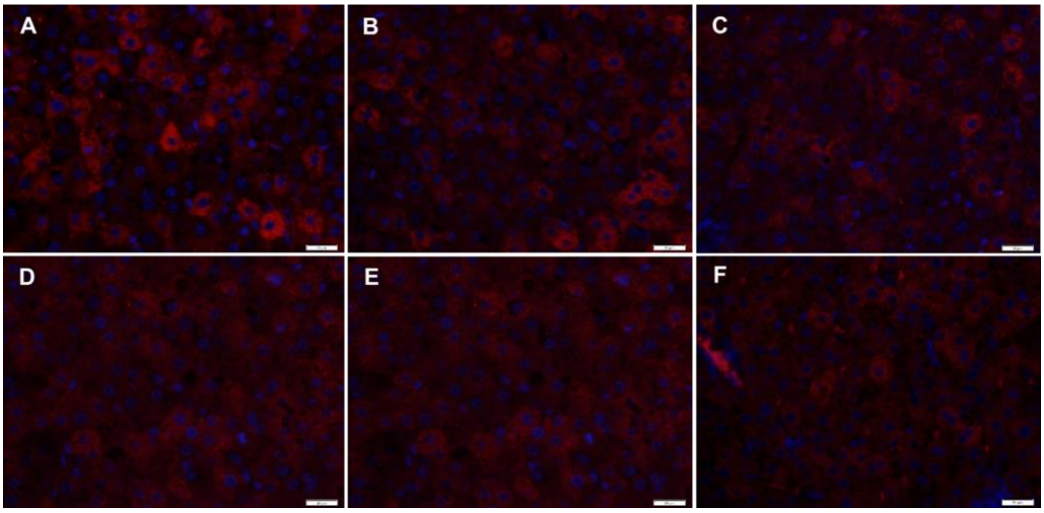

FIGURE 8. Representative immunofluorescence stain CYP1A2 in liver sections from 21-day old rats exposed to 14 days of IH and 7 days of IHR, and exposed to 2 (A), 4 (B), 6 (C), 8 (D), 10 (E), and 12 (F) IH episodes per day. CYP1A2 was significantly decreased in all areas of the liver. Images are 40× magnification. Scare bar represents 20 µm (note: refer to Figure 3E for control).

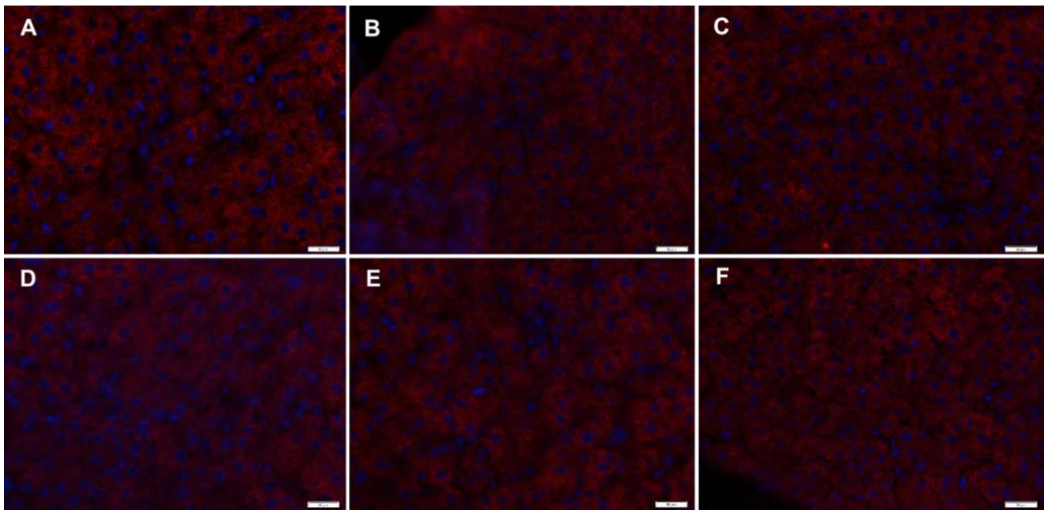

FIGURE 9. Representative immunofluorescence stain CYP2D6 in liver sections from 21-day old rats exposed to 14 days of IH and 7 days of IHR, and exposed to 2 (A), 4 (B), 6 (C), 8 (D), 10 (E), and 12 (F) IH episodes per day. CYP2D6 was significantly decreased in all areas of the liver. Images are 40× magnification. Scare bar represents 20 µm (note: refer to Figure 3D for control).

CYP isozymes undergo uncoupled catalytic turnover, resulting in the formation of superoxide, H_2O_2, and singlet oxygen [32, 54, 55]. Thus, while CYP enzymes play important roles in maintaining thera-

TABLE 1. DNA damage genes in the rat liver after 14 days of IH

Genes of Interest	4 IH Cycles/Day	6 IH Cycles/Day	8 IH Cycles/Day	10 IH Cycles/Day
Apex	11.9	3.6	7.8	14
Brca1	7	4.2	9.2	14.6
Ercc2	5.3	2.3	39.2	4.7
Hprt1	6.5	22	16.4	18.3
Mare	24.3	79.5	5.7	39.6
Mbd4	7.4	8.5	7.5	10
Mgmt	2.8	9.3	1.4	6.7
Mif	4.7	29.0	2	12.3
Msh2	10	29	4.3	15.5
Msh3	8.2	14.6	15.8	15.7
P53	4.7	3.7	4.1	8.6
Parp1	2.8	3.5	3.8	7
Rad1	5.1	10.1	2.2	14.5
Rad21	3.2	3.9	1.7	10.1
Rad23a	4.6	8.9	2.1	6.8
Rad51	3.1	11.3	12	7
Rad51c	2.6	9.2	2.1	5.5
Ube2a	3.4	11.7	3.1	9.4

Note: Data are fold change from P14 RA control. All data were corrected using 5 different housekeeping genes. Genes are selected from a profile of 84 genes. Genes of interest are: Apex (APEX nuclease multifunctional DNA repair enzyme 1); Brca1, (breast cancer 1); Ercc2 (excision repair cross-complementing rodent repair); Hprt1 (hypopxanthine phosphoribosyltransferase 1); Mare (alpha globin regulatory element containing gene); Mbd4 (methyl-CpG binding domain protein 4); Mgmt (O-6-methylguanine-DNA methyltransferase); Mif (macrophage migration inhibitory factor); Msh2 (MutS homolog 2); Msh3 ((MutS homolog 3); P53 (tumor suppressor protein 53); Parp 1 (poly ADP-ribose polymerase 1); Rad 1, 21, 23a, 51, 51c (RAD1, 21, 23a, 51, 51c homolog); Ube2a (ubiquitin-conjugating enzyme E2A).

peutic level of a drug in the body, they continuously produce ROS as an inevitable result of oxidative drug metabolism. Adverse drug effects are also attributable to CYP ROS generation. ROS disrupted CYP1A2 and contributed to acetaminophen liver toxicity [21] and theophylline metabolism [27].

Superoxide dismutase (SOD) is the first line of defense against superoxide anion, and is the primary ROS detoxifying enzyme [56]. Three forms of SOD exist in the cell, namely, copper-and zinc containing

SOD (CuZnSOD, or SOD-1), manganese-containing SOD (MnSOD, or SOD-2); and extracellular SOD (ECSOD, or SOD-3) [57]. All forms of SOD catalyze the dismutation of superoxide anion into H_2O_2 and O_2. The levels of SOD fluctuate in response to the amount of superoxide anion. The cell uses multiple enzyme systems to catalyze the decomposition of H_2O_2 into water and O_2. One of the systems involves glutathione peroxidase (GPx), two forms of which have been identified in mitochondria [57, 58]. Catalase is another important enzyme used by cells to decompose H_2O_2 [59, 60]. Catalase is found primarily in peroxisomes, but can also be present in the cytoplasm. In our study, it was interesting to note that as SOD levels decreased with increasing IH, the levels of catalase increased. These findings clearly demonstrate that accumulation of H_2O_2 with higher IH episodes may be the predominant ROS, as previously demonstrated by our group [34], which may be responsible for the lipid peroxidation, reduction in the expression of phase 1 metabolizing enzymes, and damage to the liver [61].

Our study found that the younger newborn rats at 7 days had more tissue damage compared to the older

TABLE 2. DNA damage genes in the 21-day old rat liver after 14 days of IH and 7 days of IHR

Genes of Interest	4 IH Cycles/Day	6 IH Cycles/Day	8 IH Cycles/Day	10 IH Cycles/Day
Apex	–1.8	1.5	2.6	1.5
Brca1	1.2	–3.9	1.9	1.5
Ercc2	–2.9	–1.3	–1.3	–3.9
Hprt1	1.9	1.3	13.1	5.9
Mare	–1.8	–1.5	2.5	1.3
Mbd4	–1.2	–1.1	1.3	1.1
Mgmt	–2.6	–4.9	2.1	1.3
Mif	–1.4	–3	2	1.1
Msh2	–1.8	1.1	1.5	1.2
Msh3	–1.6	–1.5	2.4	1.1
P53	–1.1	–1.4	2.3	2.2
Parp1	–1.6	–1.5	–1.2	–1.1
Rad1	–1.9	–1.4	2.6	1
Rad21	–1.7	3.5	5.3	1.9
Rad23a	–1.8	–1.7	–1	–1
Rad51	–1.6	–2.3	2	1.8
Rad51c	–2	1	2.1	–1
Ube2a	–1.7	1.0	3.9	2.1

Note: Data are fold change from P21 RA control. Genes of interest are as described in Table 1. Downregulated genes are presented with a minus sign.

rats at P14 and P21, suggesting tissue repair and regeneration in the older rats. This is evident by the increased expression of genes that regulate DNA damage and repair. Over 90% of all ELGANs are treated with caffeine for AOP. Caffeine is metabolized in the liver primarily by CYP1A2, which accounts for 95% of caffeine clearance. CYP1A2 is developmentally delayed in human fetal liver and is the last major CYP isoform to develop during the first postnatal trimester [62]. Some 25% of all clinically used drugs are metabolized by CYP2D6 [63], several of which are commonly used in newborns and neonates [46]. However, like CYP1A2, CYP2D6 is increased after birth [64]. For these reasons, we examined the expression of CYP1A2 and CYP2D6 in the P21 rats only and found that exposure to IH, even at low numbers of episodes, suppresses the expression of both CYP1A2 and CYP2D6 in the liver. The consequences of this can have major implications in the preterm infant such as therapeutic failure and toxicity.

One of the most significant findings was the robust expression of aldehyde dehydrogenases (Aldh), particularly Aldh6 after 14 days of 10 IH episodes per day, and to a greater extent at P21, after 7 days of IHR. Aldehydes are generated during a series of physiological processes with more than 200 aldehyde species arising from lipid peroxidation [64]. Aldehydes are detoxified by Aldh which protects the cells against lipid peroxidation. The upregulation of Aldh during increased IH episodes may represent a compensatory response to counteract increasing lipid peroxidation in the liver. To our knowledge, this is the first study to demonstrate this phenomenon, and these data suggest that Aldh may represent a novel therapeutic target against lipid peroxidation. Another interesting finding was the increased expression of Cyp2c22 and Cyp2e1 after chronic IH exposure. The liver contains abundant members of CYP2C family metabolizing drugs such as paclitaxel (CYP2C8) and NSAIDs (CYP2C9). CYP2C22, sharing 80% similarity with CYP2C9, is predominantly expressed in the liver, and is involved in retinoic acid metabolism [64]. Interestingly, retinoic acid is also involved in oxidative stress [65]. CYP2E1 is also intimately involved in oxidative stress in the liver [66], and de-

TABLE 3. Phase 1 drug metabolizing genes in the rat liver after 14 days of IH

Genes of Interest	4 IH Cycles/Day	6 IH Cycles/Day	8 IH Cycles/Day	10 IH Cycles/Day
Aldh1a1	22.2	9.5	4.0	28.6
Aldh2	32.3	83.3	3.0	41.8
Aldh4	41.7	45.3	10.3	60.3*
Aldh5a1	19.9	32.6	4.2	23.0
Aldh6	21.8	64.8	8.9	139.3*
Aldh8a1	44.8	34.0	7.5	22.2
COX-1	15.9	19.7	2.5	34.6*
COX-2	3.2	2.0	1.2	14.3*
Cyp1a1	4.7	1.8	1.5	12.5
Cyp1a2	12.8	9.1	2.2	13.6
Cyp2a3	10.0	21.2	5.3	28.1
Cyp2b2	33.2	60.0	2.0	38.0
Cyp2c11	22.4	43.3	4.1	16.8
Cyp2c22	20.5	77.1	–2.1	34.0
Cyp2c23	12.1	34.5	4.2	15.3
Cyp2d2	7.1	2.6	0	1.9
Cyp2d4	9.1	19.9	1.8	17.6
Cyp2e1	35.7	39.0	11.8	47.3*
Cyp2f4	24.1	11.2	3.4	16.4
Cyp8b1	82.6	65.4	6.1	9.5
Fmo1	77.7	26.2	13.6	19.6*
Fmo5	33.9	34.9	3.6	62.1*
Xdh	2.7	3.8	–1.8	8.7

*Note: Data are fold change from P14 RA control. Genes of interest are: aldh1a1 (aldehyde dehydrogenase 1 family, member A1); aldh2 (aldehyde dehydrogenase 2 family, mitochondrial); aldh4 (alcohol dehydrogenase 4 (class II), pi polypeptide); aldh5a1 (aldehyde dehydrogenase 5 family, member A1); aldh6 (alcohol dehydrogenase 6, class V); aldh8a1 (aldehyde dehydrogenase 8 family, member A1); COX-1 (cyclooxygenase 1); COX-2 (cyclooxygenase 2); Cyp1a1, 1a2 (cytochrome P450, family 1, subfamily a, polypeptide 1, 2); Cyp2a3 (cytochrome P450, family 2, subfamily a, polypeptide 3); Cyp2b2 (cytochrome P450, family 2, subfamily b, polypeptide 2); Cyp2c11, 22, 23 (cytochrome P450, family 2, subfamily c, polypeptide 11, 22, 23); Cyp2d2, 4 (cytochrome P450, family 2, subfamily d, polypeptide 2, 4); Cyp2e1 (cytochrome P450, family 2, subfamily e, polypeptide 1); Cyp2f4 (cytochrome P450, family 2, subfamily f, polypeptide 4); Cyp8b1 (cytochrome P450, family 8, subfamily b, polypeptide 1); Fmol1, 5 (flavin containing monooxygenase 1, 5); Xdh (xanthine dehydrogenase). Downregulated genes are presented with a minus sign. *genes associated with lipid peroxidation and inflammation.*

velopment of steatosis and apoptosis [67]. Taken together, these findings clearly indicate that increasing IH is closely associated with hepatic lipid peroxidation, which may not be ameliorated but further enhanced by IHR.

In conclusion, the liver appears to be tolerant of short-term, but not prolonged IH exposure. Less IH events produced more SOD possibly in response to increased superoxide anion, while more IH events produced more catalase which may indicate accumulation of H_2O_2. Long-term IH events produced more severe oxidative stress and DNA damage. This may have implications for preterm infants who have immature drug metabolizing systems, experience fre-

TABLE 4. Phase 1 drug metabolizing genes in the 21-day old rat liver after 14 days of IH and 7 days of IHR

Genes of Interest	4 IH Cycles/Day	6 IH Cycles/Day	8 IH Cycles/Day	10 IH Cycles/Day
Aldh1a1	5.4	10.6	7.2	14.2
Aldh2	7.4	7.7	5.3	59.1*
Aldh4	6.8	1.9	4.5	20.2*
Aldh5a1	6.2	3.5	6.8	19.1*
Aldh6	47.3	21.7	7.5	230.7*
Aldh8a1	4.4	4.9	4.5	9.7
COX-1	1.8	4.7	2.7	24.3
COX-2	2.1	15.0	21.6	28.7*
Cyp1a1	18.0	3.3	4.1	4.8
Cyp1a2	5.5	–1.3	1.6	4.5
Cyp2a3	10.7	–1.0	6.1	8.1
Cyp2b2	4.1	1.3	4.0	7.9
Cyp2c22	15.5	11.5	8.9	86.8*
Cyp2c23	13.1	1.2	5.2	21.8
Cyp2d2	–1.2	–1.4	–1.9	–2.1
Cyp2d4	4.7	1.0	2.4	15.4
Cyp2e1	18.0	1.8	2.4	60.6*
Cyp2f4	6.3	11.1	4.1	15.0
Cyp8b1	9.4	1.9	5.0	2.8
Fmo1	13.1	6.6	3.9	12.9
Fmo5	8.0	5.5	4.3	35.4*
Xdh	2.7	1.5	4.3	10.1

*Note: Data are fold change from P21 RA control animals. Genes of interest are as described in Table 3. Downregulated genes are presented with a minus sign. *genes associated with lipid peroxidation and inflammation.*

quent oxygen desaturations and apneas during oxygen therapy, and exposed to numerous off-label drugs. Finally, suppression of key genes responsible for metabolism of drugs commonly used in the preterm neonate in the setting of IH may be orchestrated by H_2O_2, a master contributor to lipid peroxidation, and possibly, other toxic reactions.

ACKNOWLEDGMENTS

This work was supported by the National Institutes of Health–Eunice Kennedy Shriver National Institute of Child Health and Human Development, Bethesda MD, USA (Grant No. 1U54HD071594). Authors declare no conflicts of interest related to the work reported in this paper.

REFERENCES

1. Burke BL, Robbins JM, Bird TM, Hobbs CA, Nesmith C, Tilford JM. Trends in hospitalizations for neonatal jaundice and kernicterus in the United States, 1988–2005. *Pediatrics* 2009; 123(2):524–32. doi: 10.1542/peds.2007–2915.
2. Christensen RD, Henry E, Wiedmeier SE, Burnett J, Lambert DK. Identifying patients, on the first day of life, at high-risk of developing parenteral nutrition-associated liver disease. *J Perinatol* 2007; 27(5):284–90. doi: 10.1038/sj.jp.7211686.
3. Stewart SM, Uauy R, Kennard BD, Waller DA, Benser M, Andrews WS. Mental development and growth in children with chronic liver disease

of early and late onset. *Pediatrics* 1988; 82(2):167–72.
4. Zhao J, Gonzalez F, Mu D. Apnea of prematurity: from cause to treatment. *Eur J Pediatr* 2011; 170(9):1097–105. doi: 10.1007/s00431-011-1409-6.
5. Upton CJ, Milner AD, Stokes GM. Apnoea, bradycardia, and oxygen saturation in preterm infants. *Arch Dis Child* 1991; 66(4 Spec No):381–5.
6. Martin RJ, Wang K, Koroglu O, Di Fiore J, Kc P. Intermittent hypoxic episodes in preterm infants: do they matter? *Neonatology* 2011; 100(3):303–10. doi: 10.1159/000329922.
7. Martin RJ, Di Fiore JM, Macfarlane PM, Wilson CG. Physiologic basis for intermittent hypoxic episodes in preterm infants. *Adv Exp Med Biol* 2012; 758:351–8. doi: 10.1007/978-94-007-4584-1_47.
8. Di Fiore JM, Bloom JN, Orge F, Schutt A, Schluchter M, Cheruvu VK, et al. A higher incidence of intermittent hypoxemic episodes is associated with severe retinopathy of prematurity. *J Pediatr* 2010; 157(1):69–73. doi: 10.1016/j.jpeds.2010.01.046.
9. Inayat M, Bany-Mohammed F, Valencia A, Tay C, Jacinto J, Aranda JV, et al. Antioxidants and biomarkers of oxidative stress in preterm infants with symptomatic patent ductus arteriosus. *Am J Perinatol* 2015; 32(9):895–904. doi: 10.1055/s-0035-1544948.
10. Davis JM, Auten RL. Maturation of the antioxidant system and the effects on preterm birth. *Semin Fetal Neonatal Med* 2010; 15(4):191–5. doi: 10.1016/j.siny.2010.04.001.
11. Baba L, McGrath JM. Oxygen free radicals: effects in the newborn period. *Adv Neonatal Care* 2008; 8(5):256–64. doi: 10.1097/01.ANC.0000338015.25911.8a.
12. Hirano K, Morinobu T, Kim H, Hiroi M, Ban R, Ogawa S, et al. Blood transfusion increases radical promoting non-transferrin bound iron in preterm infants. *Arch Dis Child Fetal Neonatal Ed* 2001; 84(3):F188–93.
13. Lackmann GM, Schnieder C, Bohner J. Gestational age-dependent reference values for iron and selected proteins of iron metabolism in serum of premature human neonates. *Biol Neonate* 1998; 74(3):208–13.
14. Siimes MA, Addiego JE, Jr., Dallman PR. Ferritin in serum: diagnosis of iron deficiency and iron overload in infants and children. *Blood* 1974; 43(4):581–90.
15. Wardle SP, Drury J, Garr R, Weindling AM. Effect of blood transfusion on lipid peroxidation in preterm infants. *Arch Dis Child Fetal Neonatal Ed* 2002; 86(1):F46–8.
16. Gitto E, Reiter RJ, Karbownik M, Tan DX, Gitto P, Barberi S, et al. Causes of oxidative stress in the pre- and perinatal period. *Biol Neonate* 2002; 81(3):146–57. doi: 51527.
17. Gitto E, Marseglia L, Manti S, D'Angelo G, Barberi I, Salpietro C, et al. Protective role of melatonin in neonatal diseases. *Oxid Med Cell Longev* 2013; 2013:980374. doi: 10.1155/2013/980374.
18. Kalogeris T, Baines CP, Krenz M, Korthuis RJ. Cell biology of ischemia/reperfusion injury. *Int Rev Cell Mol Biol* 2012; 298:229–317. doi: 10.1016/B978-0-12-394309-5.00006-7.
19. Kalogeris T, Bao Y, Korthuis RJ. Mitochondrial reactive oxygen species: a double edged sword in ischemia/reperfusion vs preconditioning. *Redox Biol* 2014; 2:702–14. doi: 10.1016/j.redox.2014.05.006.
20. Feng SZ, Tian JL, Zhang Q, Wang H, Sun N, Zhang Y, et al. An experimental research on chronic intermittent hypoxia leading to liver injury. *Sleep Breath* 2011; 15(3):493–502. doi: 10.1007/s11325-010-0370-3.
21. Savransky V, Reinke C, Jun J, Bevans-Fonti S, Nanayakkara A, Li J, et al. Chronic intermittent hypoxia and acetaminophen induce synergistic liver injury in mice. *Exp Physiol* 2009; 94(2):228–39. doi: 10.1113/expphysiol.2008.044883.
22. Jun J, Savransky V, Nanayakkara A, Bevans S, Li J, Smith PL, et al. Intermittent hypoxia has organ-specific effects on oxidative stress. *Am J Physiol Regul Integr Comp Physiol* 2008; 295(4):R1274–81. doi: 10.1152/ajpregu.90346.2008.
23. Savransky V, Bevans S, Nanayakkara A, Li J, Smith PL, Torbenson MS, et al. Chronic intermittent hypoxia causes hepatitis in a mouse model of diet-induced fatty liver. *Am J Physiol Gastrointest Liver Physiol* 2007; 293(4):G871–7. doi: 10.1152/ajpgi.00145.2007.
24. Novak DA, Suchy F, Balistreri W. Disorders of the liver and biliary system relevant to clinical

practice. In: *Osk's Pediatrics: Principles and Practice* (JA McMillan). 3rd Edition. Lipincott, Williams & Wilkins, Philadelphia, PA, USA. 1999. pp. 1714–37.
25. Vij AG, Kishore K, Dey J. Effect of intermittent hypobaric hypoxia on efficacy & clearance of drugs. *Indian J Med Res* 2012; 135:211–6.
26. Savransky V, Nanayakkara A, Vivero A, Li J, Bevans S, Smith PL, et al. Chronic intermittent hypoxia predisposes to liver injury. *Hepatology* 2007; 45(4):1007–13. doi: 10.1002/hep.21593.
27. Chen XY, Zeng YM, Zhang YX, Wang WY, Wu RH. Effect of chronic intermittent hypoxia on theophylline metabolism in mouse liver. *Chin Med J (Engl)* 2013; 126(1):118–23.
28. Aranda JV, MacLeod SM, Renton KW, Eade NR. Hepatic microsomal drug oxidation and electron transport in newborn infants. *J Pediatr* 1974; 85(4):534–42.
29. Allegaert K, van de Velde M, van den Anker J. Neonatal clinical pharmacology. *Paediatr Anaesth* 2014; 24(1):30–8. doi: 10.1111/pan.12176.
30. Allegaert K, Rayyan M, Vanhaesebrouck S, Naulaers G. Developmental pharmacokinetics in neonates. *Expert Rev Clin Pharmacol* 2008; 1(3):415–28. doi: 10.1586/17512433.1.3.415.
31. Barker CW, Fagan JB, Pasco DS. Down-regulation of P4501A1 and P4501A2 mRNA expression in isolated hepatocytes by oxidative stress. *J Biol Chem* 1994; 269(6):3985–90.
32. Yasui H, Hayashi S, Sakurai H. Possible involvement of singlet oxygen species as multiple oxidants in p450 catalytic reactions. *Drug Metab Pharmacokinet* 2005; 20(1):1–13.
33. El-Kadi AO, Bleau AM, Dumont I, Maurice H, du Souich P. Role of reactive oxygen intermediates in the decrease of hepatic cytochrome P450 activity by serum of humans and rabbits with an acute inflammatory reaction. *Drug Metab Dispos* 2000; 28(9):1112–20.
34. Beharry KD, Cai CL, Sharma P, Bronshtein V, Valencia GB, Lazzaro DR, et al. Hydrogen peroxide accumulation in the choroid during intermittent hypoxia increases risk of severe oxygen-induced retinopathy in neonatal rats. *Invest Ophthalmol Vis Sci* 2013; 54(12):7644–57. doi: 10.1167/iovs.13-13040.
35. Aranda JV, Cai CL, Ahmad T, Bronshtein V, Sadeh J, Valencia GB, et al. Pharmacologic synergism of ocular ketorolac and systemic caffeine citrate in rat oxygen-induced retinopathy. *Pediatr Res* 2016; 80(4):554–65. doi: 10.1038/pr.2016.105.
36. Tu C, Beharry KD, Shen X, Li J, Wang L, Aranda JV, et al. Proteomic profiling of the retinas in a neonatal rat model of oxygen-induced retinopathy with a reproducible ion-current-based MS1 approach. *J Proteome Res* 2015; 14(5):2109–20. doi: 10.1021/pr501238m.
37. Jivabhai Patel S, Bany-Mohammed F, McNally L, Valencia GB, Lazzaro DR, Aranda JV, et al. Exogenous Superoxide dismutase mimetic without scavenging H_2O_2 causes photoreceptor damage in a rat model for oxygen-induced retinopathy. *Invest Ophthalmol Vis Sci* 2015; 56(3):1665–77. doi: 10.1167/iovs.14-15321.
38. Chang M, Bany-Mohammed F, Kenney MC, Beharry KD. Effects of a superoxide dismutase mimetic on biomarkers of lung angiogenesis and alveolarization during hyperoxia with intermittent hypoxia. *Am J Transl Res* 2013; 5(6):594–607.
39. Brock RS, Gebrekristos BH, Kuniyoshi KM, Modanlou HD, Falcao MC, Beharry KD. Biomolecular effects of JB1 (an IGF-I peptide analog) in a rat model of oxygen-induced retinopathy. *Pediatr Res* 2011; 69(2):135–41. doi: 10.1203/PDR.0b013e318204e6fa.
40. Coleman RJ, Beharry KD, Brock RS, Abad-Santos P, Abad-Santos M, Modanlou HD. Effects of brief, clustered versus dispersed hypoxic episodes on systemic and ocular growth factors in a rat model of oxygen-induced retinopathy. *Pediatr Res* 2008; 64(1):50–5. doi: 10.1203/PDR.0b013e31817307ac.
41. Yaffe SJ, Aranda JV. *Neonatal and Pediatric Pharmacology: Therapeutic Principles in Practice.* 4th Edition. Lipincott, Williams & Wilkins, Philadelphia, PA, USA. 2011.
42. Allegaert K, Verbesselt R, Naulaers G, van den Anker JN, Rayyan M, Debeer A, et al. Developmental pharmacology: neonates are not just small adults. *Acta Clin Belg* 2008; 63(1):16–24. doi: 10.1179/acb.2008.003.
43. Robertson AF. Reflections on errors in neonatology III. The "experienced" years, 1970 to 2000. *J Perinatol* 2003; 23(3):240–9. doi: 10.1038/sj.jp.7210873.
44. Treluyer JM, Cheron G, Sonnier M, Cresteil T.

Cytochrome P-450 expression in sudden infant death syndrome. *Biochem Pharmacol* 1996; 52(3):497–504.
45. Treluyer JM, Gueret G, Cheron G, Sonnier M, Cresteil T. Developmental expression of CYP2C and CYP2C-dependent activities in the human liver: in-vivo/in-vitro correlation and inducibility. *Pharmacogenetics* 1997; 7(6):441–52.
46. Treluyer JM, Jacqz-Aigrain E, Alvarez F, Cresteil T. Expression of CYP2D6 in developing human liver. *Eur J Biochem* 1991; 202(2):583–8.
47. Morselhi PL. Clinical pharmacokinetics in neonates. *Clin Pharmacokinet* 1976; 1:81–98.
48. de Wildt SN, Kearns GL, Leeder JS, van den Anker JN. Cytochrome P450 3A: ontogeny and drug disposition. *Clin Pharmacokinet* 1999; 37(6):485–505. doi: 10.2165/00003088-199937060-00004.
49. Windorfer A, Kuenzer W, Urbanek R. The influence of age on the activity of acetylsalicylic acid-esterase and protein-salicylate binding. *Eur J Clin Pharmacol* 1974; 7(3):227–31.
50. Di Toro R, Lupi L, Ansanelli V. Glucuronation of the liver in premature babies. *Nature* 1968; 219(5151):265–7.
51. Drummond GS, Kappas A. An experimental model of postnatal jaundice in the suckling rat: suppression of induced hyperbilirubinemia by Sn-protoporphyrin. *J Clin Invest* 1984; 74(1):142–9. doi: 10.1172/JCI111394.
52. Milne GL, Yin H, Brooks JD, Sanchez S, Jackson Roberts L, 2nd, Morrow JD. Quantification of F2-isoprostanes in biological fluids and tissues as a measure of oxidant stress. *Methods Enzymol* 2007; 433:113–26. doi: 10.1016/S0076-6879(07)33006-1.
53. Morrow JD. The isoprostanes - unique products of arachidonate peroxidation: their role as mediators of oxidant stress. *Curr Pharm Des* 2006; 12(8):895–902.
54. White RE, Coon MJ. Oxygen activation by cytochrome P-450. *Annu Rev Biochem* 1980; 49:315–56. doi: 10.1146/annurev.bi.49.070180.001531.
55. Bae YS, Oh H, Rhee SG, Yoo YD. Regulation of reactive oxygen species generation in cell signaling. *Mol Cells* 2011; 32(6):491–509. doi: 10.1007/s10059-011-0276-3.
56. Zelko IN, Mariani TJ, Folz RJ. Superoxide dismutase multigene family: a comparison of the CuZn-SOD (SOD1), Mn-SOD (SOD2), and EC-SOD (SOD3) gene structures, evolution, and expression. *Free Radic Biol Med* 2002; 33(3):337–49. doi: 10.1016/S0891-5849(02)00905-X
57. Esworthy RS, Ho YS, Chu FF. The Gpx1 gene encodes mitochondrial glutathione peroxidase in the mouse liver. *Arch Biochem Biophys* 1997; 340(1):59–63. doi: 10.1006/abbi.1997.9901.
58. Maiorino M, Scapin M, Ursini F, Biasolo M, Bosello V, Flohe L. Distinct promoters determine alternative transcription of gpx-4 into phospholipid-hydroperoxide glutathione peroxidase variants. *J Biol Chem* 2003; 278(36):34286–90. doi: 10.1074/jbc.M305327200.
59. Chelikani P, Fita I, Loewen PC. Diversity of structures and properties among catalases. *Cell Mol Life Sci* 2004; 61(2):192–208. doi: 10.1007/s00018-003-3206-5.
60. Zamocky M, Furtmuller PG, Obinger C. Evolution of catalases from bacteria to humans. *Antioxid Redox Signal* 2008; 10(9):1527–48. doi: 10.1089/ars.2008.2046.
61. Starke PE, Farber JL. Endogenous defenses against the cytotoxicity of hydrogen peroxide in cultured rat hepatocytes. *J Biol Chem* 1985; 260(1):86–92.
62. Sonnier M, Cresteil T. Delayed ontogenesis of CYP1A2 in the human liver. *Eur J Biochem* 1998; 251(3):893–8.
63. Wang D, Papp AC, Sun X. Functional characterization of CYP2D6 enhancer polymorphisms. *Hum Mol Genet* 2015; 24(6):1556–62. doi: 10.1093/hmg/ddu566.
64. Marchitti SA, Brocker C, Stagos D, Vasiliou V. Non-P450 aldehyde oxidizing enzymes: the aldehyde dehydrogenase superfamily. *Expert Opin Drug Metab Toxicol* 2008; 4(6):697–720. doi: 10.1517/17425255.4.6.697.
65. Conte da Frota ML, Jr., Gomes da Silva E, Behr GA, Roberto de Oliveira M, Dal-Pizzol F, Klamt F, et al. All-trans retinoic acid induces free radical generation and modulate antioxidant enzyme activities in rat sertoli cells. *Mol Cell Biochem* 2006; 285(1–2):173–9. doi: 10.1007/s11010-005-9077-3.
66. Mahli A, Thasler WE, Patsenker E, Muller S,

Stickel F, Muller M, et al. Identification of cytochrome CYP2E1 as critical mediator of synergistic effects of alcohol and cellular lipid accumulation in hepatocytes in vitro. *Oncotarget* 2015; 6(39):41464–78. doi: 10.18632/oncotarget.6203.

67. Abdelmegeed MA, Choi Y, Ha SK, Song BJ. Cytochrome P450-2E1 promotes aging-related hepatic steatosis, apoptosis and fibrosis through increased nitroxidative stress. *Free Radic Biol Med* 2016; 91:188–202. doi: 10.1016/j.freeradbiomed.2015.12.016.